RSC Advances

ROYAL SOCIETY OF CHEMISTRY

www.rsc.org/advances

Journal Name

RSCPublishing

ARTICLE

The effect of mesoporous silica nanoparticles surface chemistry and concentration on the α-synuclein fibrillation

Cite this: DOI: 10.1039/x0xx00000x

Received 00th January 2012,
Accepted 00th January 2012

DOI: 10.1039/x0xx00000x

www.rsc.org/

Nayyere Taebnia,[ab] Dina Morshedi,*[a] Mohsen Doostkam,[a] Soheila Yaghmaei,[b] Farhang Ali-Akbari,[a] Gurvinder Singh,[c] and Ayyoob Arpanaei*[a]

The aggregation of an amyloid protein, α-synuclein (α-Syn), has been suggested as a potential cause of Parkinson's and several other neurodegenerative diseases. To explore the possibility of using nanoparticle-based therapeutic agents for the treatment of such diseases, we investigated the influence of surface chemistry and concentration of mesoporous silica nanoparticles (MSNPs) on the fibrillation of recombinant human α-Syn protein in the present work. Bare MSNPs as well as MSNPs of different surface functionalities, including 3-(2-aminoethyl amino) propyltrimethoxysilane (AAS), succinic anhydride (carboxyl), and polyethyleneimine (PEI) were prepared and characterized by electron microscopy, zeta potential measurement, Brunauer-Emmett-Teller (BET) isotherms, and FT-IR analyses. The process of α-Syn fibril formation was monitored by Thioflavin T (ThT) assay, atomic force microscopy (AFM) and fluorescence microscopy imaging. The conformation of α-Syn molecules in fibrillar forms and upon adsorption onto MSNPs was investigated by circular dichroism (CD) analysis, and MTT assay was employed to evaluate the cytotoxicity effects of α-Syn fibrils on PC12 cell line in the absence and presence of MSNPs. The synthesized MSNPs were spherical and monodisperse with the average size of 83±6 nm. Our results showed that the fibril formation is reduced considerably in the presence of positively-charged MSNPs, *i.e.* AAS- and PEI-MSNPs, and is enhanced while treated with negatively-charged MSNPs, *i.e.* bare and carboxyl-MSNPs. Furthermore, it was also demonstrated that increasing the concentration of the MSNPs regardless of their surface chemistry results in greater effects on the fibril formation—promoting or inhibiting for negatively and positively-charged MSNPs respectively. Subsequently, the cytotoxicity of the formed aggregates was noticed to be significantly reduced in the presence of AAS- and PEI-MSNPs in comparison to that in the absence of these MSNPs. These results suggest that the electrostatic charges and concentration of MSNPs play important regulatory roles in the fibrillation process of α-Syn. Thus, the present study contributes towards the better understanding and control of protein fibrillation by nanoparticles which can lead to development of nanoparticle-mediated therapies.

1 Introduction

Protein fibrillation, a process by which misfolded proteins form large linear aggregates, has been linked to several human neurodegenerative disorders such as Alzheimer's and Parkinson's diseases [1]. The mechanism of fibrillation involves a number of intermediate states including nucleation, oligomerization, and subsequently, fibrils that cumulate extracellularly in the tissues and have pathogenic effects [2]. Both in *vitro* and in *vivo* studies have demonstrated that soluble and oligomeric forms of proteins possess potent neurotoxic activities and may cause the neuronal injury and cell death in human amyloid diseases [3-5]. Thus, the development of effective therapeutic strategies to control the oligomerization and fibrillation processes are necessary for the treatment of neurodegenerative disorders.

An alternative approach is the use of nanoparticles (NPs) as artificial chaperones that can provide control over the fibril formation. In recent years, the effect of different types of NPs on fibrillation process, either promoting or inhibiting, has been demonstrated [6-12]. For instance, amino-modified polystyrene NPs have both acceleration and retardation effects on the Aβ fibrillation process depending on the concentration and coverage of monomers on the particle surfaces [7]. Furthermore, NPs of different surface hydrophobicity such as co-polymeric N-isopropylacrylamide and N-tert-butylacrylamide (NIPAM-BAM) have been shown to inhibit

fibril growth by depleting the concentration of monomers through their adsorption onto the particles surface [8]. In another study, it has been revealed that co-incubation of gold NPs with insulin results in a delayed structural transformation into amyloid-like fibrils for a week [10]. Very recently, it has been shown that curcumin-functionalized gold NPs of 10-25 nm prevent amyloid fibrillation and disintegrate amyloid fibrils [11]. To date, two main mechanisms governing the NPs-protein interactions have been proposed: i) protein binding to the surface followed by conformational changes which leads to an accelerated fibril formation, and ii) protein binding onto the surface leading to a reduced solution concentration and consequently delayed or retarded fibrillation [13]. Based on previous studies, it can be inferred that surface area, composition, surface chemistry, and concentration of NPs play significant regulatory roles in controlling the fibrillation process. Therefore, the design of NPs, which possess suitable properties and can potentially be utilized to inhibit the protein fibrillation, is highly desirable.

Among all various types of NPs, mesoporous silica nanoparticles (MSNPs) present several unique features, such as large surface area, tunable pore size, facile surface multi-functionalization, as well as excellent biocompatibility and biodegradability. Due to all of these characteristics, MSNPs have received a great deal of attention in many areas of nanomedicine and biotechnology [14-18]. In spite of their excellent properties and enormous applications, the influence of MNSPs on protein fibrillation has never been investigated to the best of our knowledge. Thus, the focus of the present work is to study the influence of surface chemistry and concentration of MSNPs on the α-synuclein (α-Syn) fibrillation process. α-Syn is a small amyloidogenic protein (~14.5 kDa), which is believed to be involved in Parkinson's disease and related neurodegenerative disorders [19-22]. In this regard, we modified the surface chemistry of MSNPs, using different functional molecules, and investigated the dependency of α-Syn fibrillation process on the surface chemistry and on the concentration of synthesized MSNPs. In addition, the cytotoxicity of α-Syn aggregates was monitored by the 3-(4, 5-dimethylthiazol-2-yl)-2, 5-diphenyltetrazolium bromide (MTT) assay in the absence and presence of these MSNPs *in vitro*.

2 Experimental Section

2.1 Materials

Tetraethylorthosilicate (TEOS), cetyltrimethylammonium bromide (CTAB), 3-(2-aminoethyl amino) propyltrimethoxy-silane (AAS, 97 vol%), dimethylformamide (DMF), Succinic anhydride, Polyethyleneimine (M.W.=10000, 99%), ethanol (99.9%), hydrochloric acid, and glacial acetic acid were purchased from Merck (New York, USA). N-hydroxysuccinimide (NHS) and N-(3-dimethylaminopropyl)-N-ethylcarbodiimide hydrochloride (EDC) were received from Sigma-Aldrich (St. Louis, MO, USA). Water was deionized using Q-check controller system (OES Co., USA). Recombinant human α-Syn was supplied by National Institute of Genetic Engineering and Biotechnology (NIGEB).

2.2 Synthesis and characterization of MSNPs

MSNPs were synthesized by our previously reported approach based on template removing method with some modifications [23]. In brief, 0.1 g of CTAB was dissolved in a mixture of 49 mL deionized water and sodium hydroxide (2 M) at 80 °C with constant stirring. Once a clear solution was obtained, 1 mL of TEOS was added in a dropwise manner, and the mixture was stirred for 2 h. In order to remove CTAB, NPs were refluxed in an alcoholic solution of hydrochloric acid with a ratio of HCl: EtOH equal to 1:10 (v/v). After 6 h, the mixture was centrifuged and the obtained product was washed. Hitachi S-5500 electron microscopy operating at 30 kV was used to acquire images of MSNPs. Brunauer-Emmett-Teller (BET) isotherms were used to determine the morphology, surface area, and pore size of MSNPs and Fourier Transform Infrared (FT-IR) spectroscopy was employed to evaluate the CTAB removal. As a control for FT-IR analysis, non-porous silica NPs were synthesized via Stöber method through which no surfactant was utilized [24]. Zeta (ζ) potential values and hydrodynamic diameters of the particles were measured using a Malvern Zetasizer Nano instrument (S90, UK) equipped with the dynamic light scattering (DLS) system.

2.3 Functionalization of MSNPs

In order to modify the surface of MSNPs through the grafting procedure 3-(2-aminoethyl amino) propyltrimethoxysilane, succinic anhydride, and polyethyleneimine were used to obtain AAS-MSNPs, carboxyl-MSNPs and PEI-MSNPs respectively. To do this, 100 mg of MSNPs was dispersed in ethanol for 10 minutes followed by addition of deionized water for hydrolysis and glacial acetic acid as the catalyst. Then, AAS was added into the reaction mixture, and the solution was stirred for 1 h at 1000 rpm. After the completion of the reaction, AAS-MSNPs were washed with ethanol and deionized water. The synthesized AAS-MSNPs were used to achieve carboxyl-MSNPs. AAS-MSNPs were washed and then well dispersed in 20 mL of DMF. At the same time, 0.2 g of succinic anhydride was dissolved in another batch of DMF (20 mL), and the solution was stirred under a nitrogen atmosphere at 1000 rpm. After 20 minutes, a solution of well-dispersed AAS-MSNPs was added to the solution of succinic anhydride in DMF, and the resultant solution was left stirring at room temperature for 24 h. The obtained carboxyl-MSNPs were washed with DMF and deionized water. It should be noted that in each part of this work, the required amounts of MSNPs were prepared and used freshly.

In order to functionalize MSNPs with PEI molecules, carboxyl-MSNPs were first dispersed in a solution of NHS (0.2 mg/mL) and EDC (1 mg/mL) in 10 mM phosphate buffered saline (PBS, pH 8). Afterwards, 1.5 mL aliquots of the obtained suspension were shaken for 7 minutes and microfuged for 3 minutes. For the functionalization process to be completed, 10 mL of PEI solution in 10 mM PBS (2 mg/mL) was added to each aliquot and the suspension was shaken for 1 h at room temperature. Finally, PEI-MSNPs were washed with PBS and deionized water.

2.4 α-Syn fibrillation tests

α-Syn fibrillation study was performed at 37 °C in the absence and presence of MSNPs with a set of solution concentrations in 1.5 mL Eppendorf tubes. Buffer stock of 25 mM Tris-Cl (pH 7.4) was added to the monomer of α-Syn to obtain a final concentration of 2 mg/mL. Before incubation with MSNPs, the solution was microfuged (10000 rpm) for 10 minutes at 4 ºC to remove any traces of pre-existing oligomers or aggregates [25, 26]. The experiments were set up for MSNPs with various functionalities and in different concentrations of each one (0, 5, 10, 50 and 100 µg/mL). Each sample with a total volume of

150 µL—containing fixed protein concentration (2 mg/mL) and different concentrations of functionalized MSNPs (0-100 µg/mL)—was shaken in a 1.5-mL Eppendorf tube at 80 rpm and 37 °C in water bath for 24 h to complete the fibrillation process. As a control, 150 µM of α-Syn was also incubated in the absence of MSNPs. Three independent experiments were performed for each sample.

2.5 Study of α-Syn fibrillation using ThT fluorescence assay, AFM and fluorescence microscopy

The fibril formation process was monitored by ThT binding and confirmed by AFM and fluorescence microscopy at the end of assembly reaction. ThT is a dye that specifically binds to amyloid aggregates, and upon binding, the quantum yield of fluorescence increases [27], thus allowing quantitative assessment of the presence of fibrillar species. The fluorescence signals were acquired in the emission range of 450-550 nm by exciting the samples at 440 nm. The experiments were performed using a Varian Cary Eclipse fluorescence spectrophotometer (Mulgrave, Australia) at room temperature. Each experimental point is an average of the fluorescence signal of three samples containing aliquots of the same solution. The MSNPs concentration was varied in the range of 0-100 µg/mL. To evaluate the morphological changes of α-Syn aggregates/fibrils in the presence of bare and functionalized MSNPs, AFM was employed. For that, samples of the incubated α-Syn were diluted 30 times in filtered deionized water. Then, small aliquots (10 µL) were deposited on freshly cleaved mica sheets. Afterwards, samples were dried and washed with deionized water. AFM imaging was performed under noncontact mode using Veeco instrument equipped with a silicon probe (CP). Fluorescence microscopy images were recorded by Ceti inverso TC100 microscope (Medline scientific, Oxon, UK). Briefly, 15 µl of the samples was added to 15 µl of ThT (500 µM), incubated for 5 min at room temperature, and then spread onto a microscopic slide.

2.6 Circular Dichroism (CD) Analysis

CD spectra of samples were obtained in the far-UV region (190–260 nm) using an AVIV 215 spectropolarimeter (Aviv Associates, Lakewood, NJ, USA) in 0.1-cm circular cuvettes at room temperature. The protein concentration of 0.1 mg/mL was used for CD analysis.

2.7 Cytotoxicity studies

Rat pheochromocytoma (PC12) cells acquired from the Pasteur institute (Tehran, Iran) were cultured in Dulbecco's modified Eagle's medium (DMEM) supplemented with 10% fetal bovine serum (FBS), 100 units/mL penicillin, and 100 µg/mL streptomycin in a 5% CO2 humidified environment at 37 °C. Cells were seeded in 96-well plates in 100 µL of media at a cell density of 10^4 cells/well. After 24 h, the old media were replaced with the fresh media containing preincubated α-Syn fibrils with and without AAS- and PEI-MSNPs. Then, cells were further incubated at 37 °C. After 24 h, a 10 µL of 5 mg/mL MTT reagent in PBS was added to each well and the incubation was continued for 4 h. Finally, 100 µL of DMSO was added and absorption at 580 nm was determined with CST Eliza reader. A following equation was used to calculate the cell viability:

$$Cell\ viability\ [\%] = (x/x_c) \times 100$$

Where x is the absorbance of cells treated with α-Syn fibrils and/or AAS- and PEI-MSNPs and x_C is the absorbance of untreated (control) cells. The cytotoxicity of AAS- and PEI-MSNPs was also assessed through a similar procedure.

3 Results and discussion

3.1 Characterization of MSNPs of various surface chemistries

Scanning electron microscopy (SEM) and bright field scanning transmission electron microscopy (BF-STEM) images show that monodisperse spherical MSNPs with an average diameter of 83±6 nm (Figure 1a) were obtained. Similar morphologies observed through STEM imaging for functionalized samples with different surface chemistries reveal the fact that the organic/polymer layers do not notably change the size and morphology of NPs (Figure 1). However, measurements through DLS technique revealed that the size of particles increases in each step through surface functionalization in the order of bare MSNPs < AAS-MSNPs < Carboxyl-MSNPs < PEI-MSNPs (Table 1). Obviously, these sizes are larger than those determined from STEM images, most likely due to the swelling of the hydrophilic polymer layers in the aqueous solution and/or aggregation of functionalized MSNPs. The hydrodynamic diameter of the bare MSNPs (112 ± 8 nm) was not observed to be much larger than that determined from the electron microscopy images (83±6 nm). However, this small difference is possibly due to the mild aggregation of the bare MSNPs.

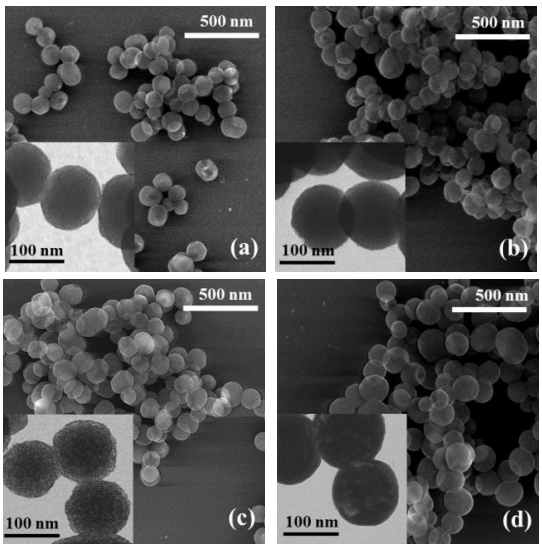

Fig.1 SEM (main) and BF-STEM (inset) images of (a) bare MSNP (b) AAS-MSNP (c) Carboxyl-MSNP (d) PEI-MSNP

The surface functionalization of MSNPs was evaluated by zeta (ζ) potential measurement (Table 1). Results show ζ potential value of -16.1 mV for bare MSNPs. However, it varies as the surface of the particles is modified with AAS, carboxyl and PEI molecules, suggesting the successful surface functionalization of NPs. These results demonstrate that, AAS-functionalized MSNPs possess positively charged surface, whereas carboxyl-functionalized MSNPs present a more negatively charged surface. Functionalization of MSNPs surface with PEI molecules, result in a more positively charged surface owing to a great number of primary, secondary and tertiary amine groups in PEI molecules.

Table 1- Zeta potential of MSNPs in aqueous solution

Sample	ζ/mV	DLS size (nm)
MSNP	-16.1	112 ± 8
AAS-MSNP	24.5	339 ± 10
Carboxyl-MSNP	-20.8	498 ± 14
PEI-MSNP	35.5	577 ± 20

FT-IR analysis was performed to ensure CTAB removal from MSNPs once treated with EtOH-HCl solution and the results were compared with controlled sample of silica nonporous NPs prepared by Stöber method which does not require any surfactant during the synthesis. FT-IR spectroscopy results indicate that the characteristic peaks (peaks in 700, 1500, 2900 and 3000 cm^{-1} for CH, CH_2 and CH_3 groups, respectively) are completely removed for the MSNPs treated with ETOH-HCl solution (Figure 2).

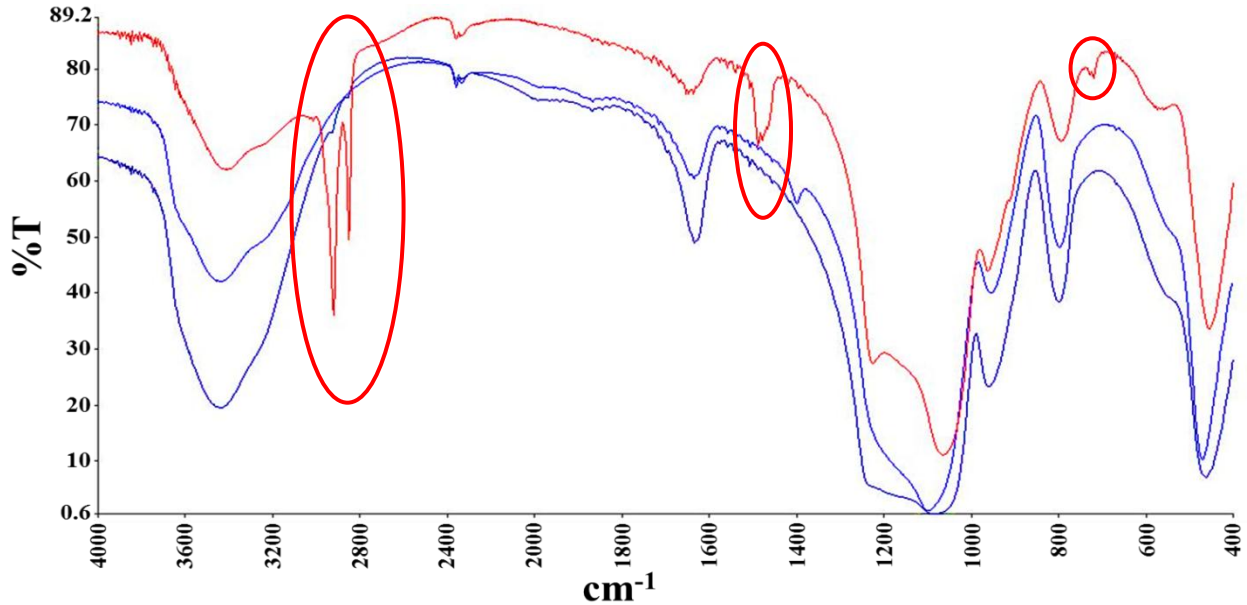

Fig.2 FTIR result of: MSNPs before CTAB removal (red), Stöber silica nanoparticles as control (blue), MSNPs after CTAB removal (purple). Insets indicate that due to presence of CH, CH_2 and CH_3 groups in CTAB molecule structure, four peaks can be observed in 700, 1500, 2900 and 3000 cm^{-1} before CTAB removal. These peaks are eliminated after treatment with EtOH-HCl.

The N_2 adsorption–desorption isotherm obtained at 77 K shows a typical type IV isotherm (Figure 3). In addition, the pore size and surface area of the MSNPs were determined to be 4.1 nm and 882.1 m^2/g respectively.

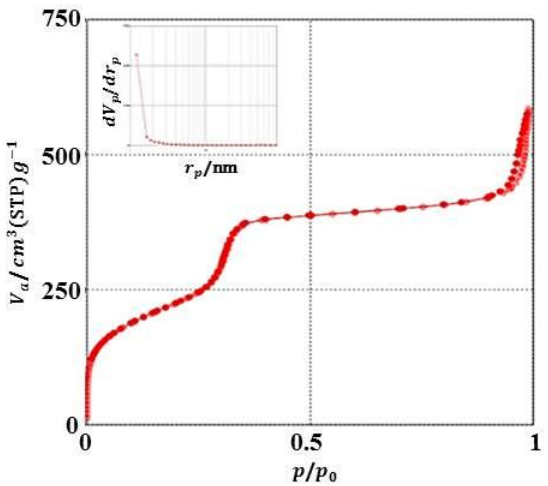

Fig.3 Type IV N_2 adsorption-desorption isotherm obtained at 77 K. The inset shows distribution of the pore size for synthesized MSNPs.

3.2 Effect of MSNPs on α-Syn fibrillation

To investigate the effect of functionalized MSNPs on the α-Syn fibrillation, the fibril formation reactions were monitored by ThT fluorescence assay, Far-UV CD spectroscopy, AFM imaging and fluorescence microscopy. α-Syn was exposed to the bare and functionalized MSNPs possessing different surface chemistries at different concentrations (0-100 μg/mL). Obtained results indicate that positively charged MSNPs, *i.e.* AAS- and PEI- MSNPs, have significant inhibitory effect on α-Syn fibrillation. On the other hand, bare MSNPs slightly enhance the fibrillation process and carboxyl-MSNPs strikingly increase the fibril formation (Figures 4). Generally, it is demonstrated that increasing the surface charge towards positive or negative values results in boosting both acceleration and retardation effects on protein fibrillation. Thus, it can be inferred that α-Syn fibrillation process depends on the surface chemistry and charge of the added MSNPs.

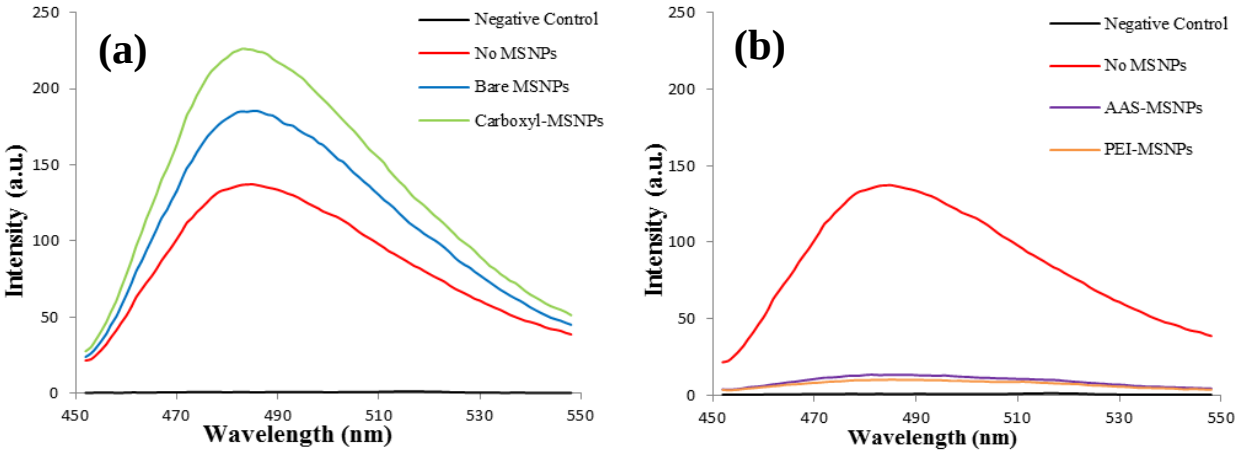

Fig.4 α-Syn fibrillation without (solid line) or with 100 μg/mL of (a) negatively charged and (b) positively charged MSNPs. Thioflavin T assay for 2 mg/mL α-Syn at 37°C and after 24 h in 25 mM Tris-Cl buffer, pH 7.4

This behavior can be understood by considering the isoelectric point of α-Syn (pI 4.74) [28], which makes this protein negatively charged in the solution used in this work (pH 7.4). Under this condition, negatively charged carboxyl-functionalized MSNPs have repulsive electrostatic interactions with α-Syn molecules. A high concentration of negatively charged moieties including α-Syn molecules and carboxyl-functionalized MSNPs can lead to enhanced depletion of soluble protein molecules through their conformational changes and consequently aggregation and fibril formation.

Figure 5 represents the results of far-UV CD spectrophotometer analysis for α-Syn protein incubated in the presence and absence of MSNPs (100 μg/mL) of different surface chemistries/surface charges. α-Syn in the monomeric form and in aqueous solutions usually has disorder structure, which can be indicated by far-UV CD spectrophotometer with a negative deep peak at 200 nm. Converting its random coil structure to the ordered crossed-β sheets causes the appearance of deep negative peaks with minima around 218 nm (Figure 5). The obtained CD data clearly show that addition of positively charged MSNPs results in completely different patterns of protein molecules conformation. In particular, these MSNPs cause a reduced β-structure content of protein molecules (Figure 5). This is more severe for PEI-MSNPs with higher ζ value in comparison to that of the AAS-MSNPs. PEI-MSNPs completely perturb the formation of β structures and cause the protein fibrils to exhibit only a smooth negative peak around 200 nm. Interestingly, the CD results reveal that the β-sheet content is strikingly increased in the presence of negatively-charged carboxyl-MSNPs compared with that in the absence of MSNPs. Bare-MSNPs do not affect the β-structure pattern of the protein molecules considerably. These results confirm the results from ThT analysis. It can be interpreted that presence of positively charged PEI-MSNPs and the resulted interactions perhaps lead α-Syn monomeric form to remain in the natural conformation upon adsorption and not to undergo the fibrillation process.

We hereby presumed that stronger electrostatic attractions between positively charged MSNPs, *i.e.* AAS- and PEI-MSNPs, and α-Syn monomers leads to the adsorption of monomers on the particle, and hence results in the protein concentration depletion and inhibition of protein fibrillation. These results are in agreement with those reported by Cabaleiro-Lago et al. demonstrating prevention of fibrillation process via adsorption of monomers and pre-fibrillar oligomers to the co-polymeric NPs [8].

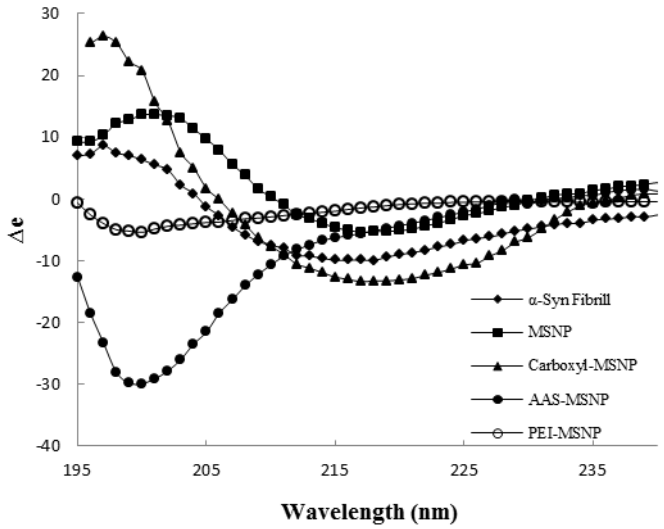

Fig.5 Far-UV CD spectrophotometer analysis of α-Syn protein incubated in the presence and absence of MSNPs owning different surface functionalities at 100 μg/mL.

However, different results were observed under the similar conditions by Lines et al. [9]. They mainly considered the effect of size and hydrophobicity of NPs surfaces. In this regard, they proposed that the protein fibrillation is enhanced in the presence of NPs due to the enrichment in the protein cluster population on the NPs of larger sizes through the association of several layers of protein with the particles [9]. They attributed these observations to the changes in structural properties of the protein through the adsorption onto hydrophobic NPs. They concluded that these changes consequently enhance the protein fibrillation. This could be due to the fact that the hydrophobic regions of the protein molecules usually are not exposed on the surface in an aqueous solvent. These regions can be exposed by protein conformational changes due to various reasons such as adsorption on the hydrophobic surfaces. Therefore, the adsorption of protein molecules on the surface of NPs may enhance the protein fibrillation if the subsequent protein conformational changes take place. In a recent investigation

kinetics of α-Syn fibrillation was found to be proportional to the amount of available hydrophobic area. It was shown that presence of polytetrafluoroethylene (PTFE) balls with their hydrophobic interface affects the aggregation process from the first hours of the experiment and agitation accelerates the fibrillation process as well [29]. Similarly, it has been demonstrated that increasing the monomer-surface interaction affects the nucleation and growth of small oligomers in a nonlinear manner. A weak interaction leads to retardation while strong interaction accelerates fibril formation [30].

Therefore, it can be concluded that if the adsorption takes place in such a way that the soluble form of protein encounters striking changes, the protein fibrillation will be enhanced. On the contrary, if the protein adsorption does not lead to any major changes in the protein conformation and its soluble form, hydrophobic regions will not be exposed on the surface and consequently the fibrillation process will be retarded due to depleting the protein concentration in the solution. This hypothesis is schematically illustrated in Figure 6.

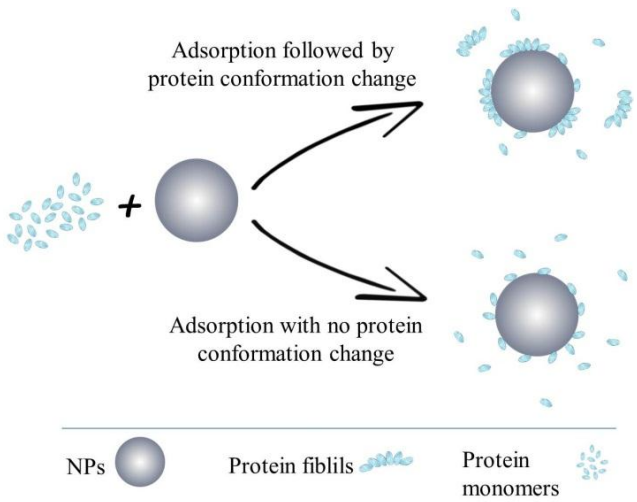

Fig.6 Two probable mechanisms for NPs-protein interaction

Our results confirm this hypothesis for the α-Syn adsorption on the AAS- and PEI-MSNPs. Mild electrostatic interactions between protein molecules and charged surfaces usually do not lead to significant changes in the protein conformation in an aqueous solvent. That is due to the fact that the electrostatic interactions take place via polar chemical groups existing on the surface of protein molecules in the aqueous media. The repulsive electrostatic interactions between protein molecules prevent their aggregation. When the concentration increases, these repulsive interactions are overcome by attractive forces, such as hydrophobic interactions. Therefore, when negatively-charged protein molecules, *i.e.* α-Syn, adsorb onto the positively-charged surfaces, *i.e.* AAS- and PEI-MSNPs, the fibrillation process is retarded due to the low protein concentration in the solution, and the protein molecules retain their conformation while the adsorption occurs.

We found that the fibrillation process is also dependent on the concentration of MSNPs. Indeed, there is a clear correlation between the investigated concentrations (0-100 µg/mL) and the rate of fibril formation (Figure 7). According to ThT results, higher concentrations of positively charged MSNPs, *i.e.* AAS- and PEI-MSNPs, lead to the lower extent of protein fibrillation, whereas higher extent of fibril formation is observed in the presence of higher concentrations of negatively charged MSNPs, *i.e.* bare and carboxyl-MSNPs (Figure 7). To facilitate the comparison between fibrillation extents, the curves are compared to the maximum intensity which belongs to pure protein.

To further confirm, AFM study was performed to investigate the effect of MSNPs on the fibril formation. These images (Figure 7) are in agreement with the results of ThT assay (Figure 4), namely they illustrate that protein fibrils are formed in less extents in the presence of AAS- and PEI-MSNPs, while their formation is enhanced in the presence of bare and carboxyl-MSNPs.In addition protein aggregates, causing induced emission of fluorescence through interaction with ThT, can be seen as highly bright particles in fluorescence microscopy images. However, they do not show fibril-like structures due to the low resolution and magnification.

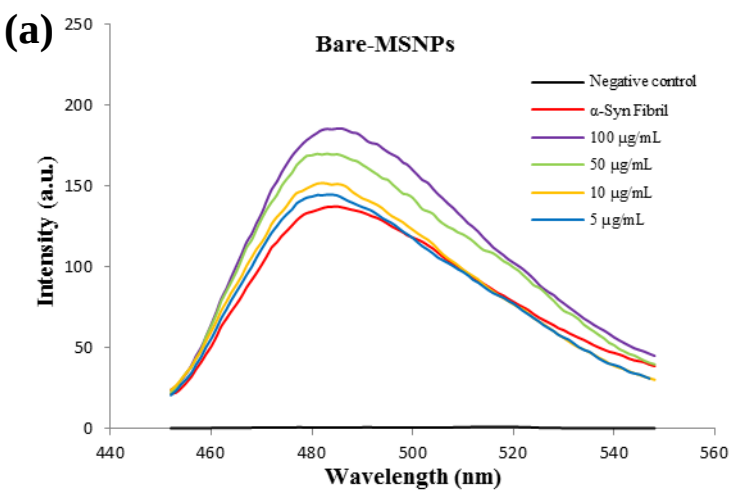

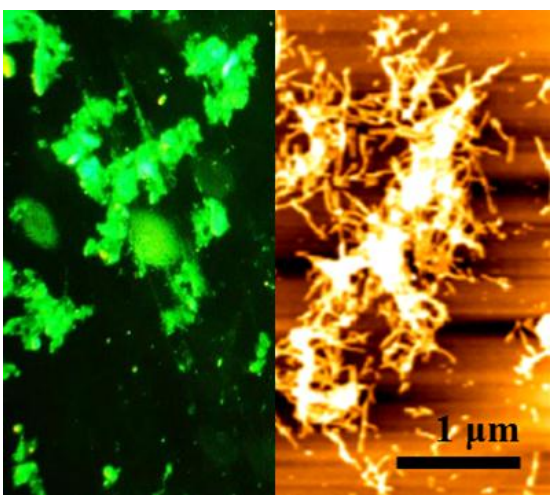

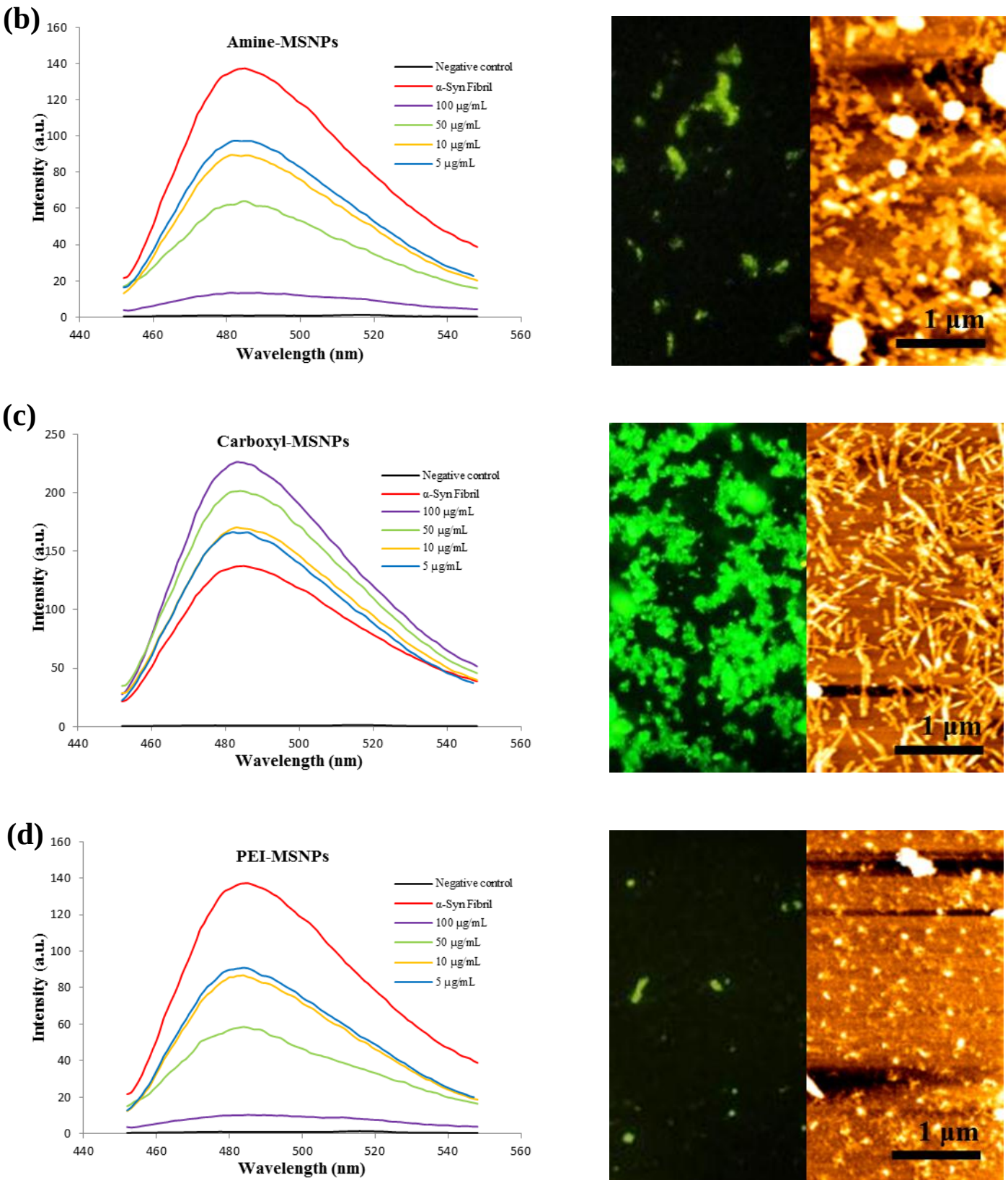

Fig.7 ThT assay results of α-Syn fibrils formed in the presence of different concentrations of (a) Bare MSNPs; (b) AAS-MSNPs; (c) PEI-MSNPs; (d) Carboxyl-MSNPs at 37°C and after 24 h (the left panel). AFM images of α-Syn fibrils and fluorescence microscopy images of α-Syn aggregates formed in the presence of the same MSNPs at the concentration of 100 µg/mL (the right panel).

3.3 The cytotoxicity of α-Syn species

The effect of MSNPs presence on the toxicity of α-Syn species was studied by the MTT test. Since AAS- and PEI-MSNPs had demonstrated inhibitory effect on the fibrillation process, the cytotoxicity studies were performed for the samples treated by these NPs.

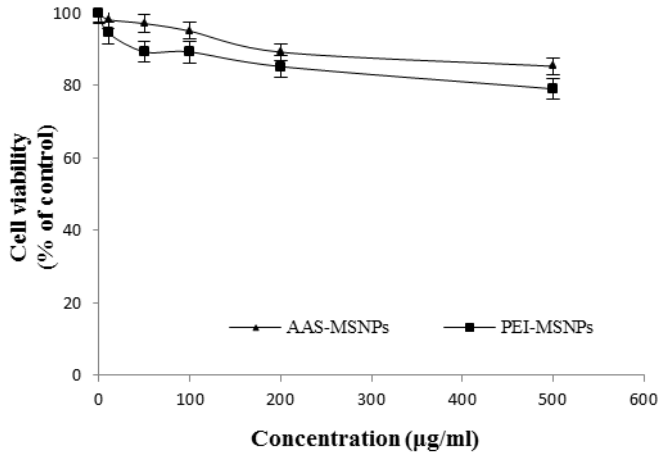

Fig.8 Changes in the cell viability on treatment with AAS- and PEI-MSNP at different concentrations

In the first step, the cytotoxicity of AAS- and PEI-MSNPs was studied. Indeed, the cell viability decreases slightly when the concentration of AAS- and PEI-MSNPs increases, but as shown in Figure 8, no considerable toxicity occurs even if high concentrations of AAS- and PEI-MSNPs (up to 500µg/mL) are used.

The cytotoxicity of α-Syn species was evaluated in the absence and presence of the AAS- and PEI-MSNPs (100 µg/mL). Obviously the toxicity of protein fibrils is significant in the absence of MSNPs, whereas lower toxicity values were observed for samples containing AAS- and PEI-MSNPs (Figure 9). The reduction of protein fibrils toxicity can be explained by considering the adsorption of α-Syn species to the surface of AAS- and PEI-MSNPs, resulting in reduced solution concentration of α-Syn monomers and delayed formation of the prefibrillar forms, which are responsible for the cytotoxicity effects of α-Syn fibrils.

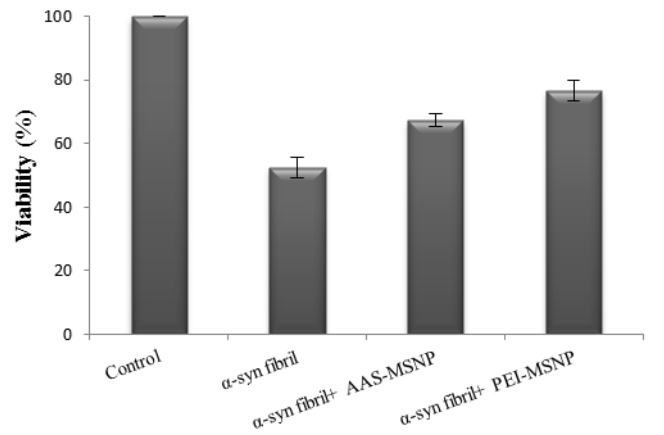

Fig.9 Changes in the cell viability upon treatment with α-Syn fibrils in the absence and presence of AAS- and PEI-MSNPs at the concentration of 100 µg/mL.

4 Conclusion

In conclusion, our results clearly reveal the great impact of surface chemistry/charge of MSNPs and their concentration on the fibrillation process of α-Syn protein. In the current investigation, AAS-and PEI-MSNPs acted as the efficient artificial chaperones and remarkably inhibited α-Syn fibrillation process. On the other hand, the bare and carboxyl-MSNPs enhanced the fibril formation. This behavior can be explained via considering the electrostatic interactions between the positively-charged (AAS- and PEI-) MSNPs and α-Syn protein molecules. Through such interactions, the absorption of α-Syn molecules onto positively-charged (AAS- and PEI-) MSNPs causes the depletion of the protein concentration in the solution and consequently, the protein fibrillation is retarded. Furthermore, the cytotoxicity effects of α-Syn species are reduced in the presence of positively-charged MSNPs. From results obtained in this study, it can be inferred that if the attractive interaction does not lead to any changes in the conformation of protein molecules and their soluble form, the fibrillation is expected to be retarded due to the protein concentration reduction in the solution. On the contrary if the interaction leads to significant changes in the conformation of the protein, it is expected that the fibrillation process is enhanced. Owing to their small sizes, allowing them to pass through different barriers in the body, MSNPs can present promising potentials for the biomedical applications in the case of protein fibrillation-based diseases. However, an important step toward this goal, which still needs to be comprehensively investigated, is to understand the role of parameters such as MSNPs size as well as kinetics of the α-Syn fibrillation process in the presence of these NPs.

Acknowledgements

This work is financially supported by Iran National Science Foundation (INFS). The authors thank NTNU Nanolab for providing instrumentation facilities. The Research Council of Norway is acknowledged for the support to the Norwegian Micro-and Nano-Fabrication Facility, NorFab (197411/V30).

Notes and references

[a] Department of Industrial and Environmental Biotechnology, National Institute of Genetic Engineering and Biotechnology (NIGEB), Tehran, Iran. E-mails: A. Arpanaei, arpanaei@yahoo.com; D. Morshedi, morshedi@nigeb.ac.ir; Tel.: +98 (21) 44787463; Fax +98 (21) 44787395.

[b] Department of Chemical and Petroleum Engineering, Sharif University of Technology, Tehran, Iran.

[c] Department of Materials Science and Engineering, Norwegian University of Science and Technology, Trondheim, Norway.

1 C.M. Dobson, *Nature*, 2003, **426**, 884-890.

2 I.F. Tsigelny, Y. Sharikov, M.A. Miller and E. Masliah, *Nanomedicine*, 2008, **4**, 350–357.

3 M.S. Goldberg and P.T. Lansbury, *Nat. Cell Biol*, 2000, **2**, 115-119.

4 B. Winner, R. Jappelli, S.K. Maji, P.A. Desplats, L. Boyer, S. Aigner, C. Hetzer, T. Loher, M. Vilar, S. Campioni, C. Tzitzilonis, A. Soragni, S. Jessberger, H. Mira, A. Consiglio, E. Pham, E. Masliah, F.H. Gage and R. Riek, *Proc Natl. Acad. Sci. (PNAS)*, 2011, **108**, 4194-4199.

5 Z.S. Martin, V. Neugebauer, K.T. Dineley, R. Kayed, W. Zhang, L.C. Reese and G. Taglialatela, *J. Neurochem*, 2012, **120**, 440-452.
6 M. Zaman , E. Ahmad, A. Qadeer, G. Rabbani and R.H. Khan, *Int. J. Nanomedicine*, 2014, **9**, 899-912.
7 C. Cabaleiro-Lago, F. Quinlan-Pluck, I. Lynch, K.A. Dawson and S. Linse, *ACS Chem. Neurosci*, 2010, **1**, 279-287.
8 C. Cabaleiro-Lago, F. Quinlan-Pluck, I. Lynch, S. Lindman, A.M. Minogue, E. Thulin, D.M. Walsh, K.A. Dawson and S. Linse, *J. Am. Chem. Soc*. *(JACS)*, 2008, **130**, 15437-15443.
9 S. Linse, C. Cabaleiro-Lago, W.F. Xue, I. Lynch, S. Lindman, E. Thulin, S.E. Radford and K.A. Dawson, *Proc. Natl. Acad. Sci. (PNAS)*, 2007, **104**, 8691-8696.
10 S. Hsieh, C.W. Chang and H.H. Chou, *Colloids Surf B Biointerfaces*, 2013, **112**, 525-529.
11 S.L. Palmal, A.R. Maity, B.K. Singh, S. Basu and N.R. Jana, *Chemistry*, 2014, **20(20)**, 6184-6191.
12 L.H. Xiao, D. Zhao, W.H. Chan, M.M.F. Choi and H.W. Li, *Biomaterials*, 2010, **31**, 91-98.
13 M. Mahmoudi, H.R. Kalhor, S. Laurent and I. Lynch, *Nanoscale*, 2013, **5**, 2570-2588.
14 S. Wang, *Microporous Mesoporous Materials*, 2009, **117**, 1-9.
15 M. Vallet-Regí, *J. Intern. Med.*, 2010, **267**, 22-43.
16 J. Salonen and V.P. Lehto, *Chem. Eng. J.*, 2010, **137**, 162-172.
17 K. Cheng and C.C. Landry, *J. Am. Chem. Soc.*, 2007, **129**, 9674-9685.
18 N. Gartmann and D. Bruhwiler, *Angew. Chem. Int. Ed.*, 2009, **48**, 6354-6356.
19 L. Breydo, J.W. Wu and V.N. Uversky, *Biochimica et Biophysica Acta*, 2012, **1822**, 261-285.
20 L. Giehm, N. Lorenzen and D.E. Otzen, *Methods*, 2011, **53**, 295‑305.
21 N. Pandey, J.V. Strider, W.C. Nolan, S.X. Yan and J.E. Galvin, *Acta Neuropathol*, 2008, **115**, 479-489.
22 M.R. Cookson, *Annu. Rev. Biochem.*, 2005, **74**, 29-52.
23 A. Arpanaei, L. Kermanshah, M. Vosoughi and H. Javadi, *Proc. of the 4th Conference on Nanostructures*, Kish Island, Iran, 2012.
24 W. Stöber, A. Fink and E. Bohn, *Journal of Colloid and Interface Science*, 1968, **26(1)**, 62-69.
25 M. Ghavami, M. Rezaei, R. Ejtehadi, M. Lotfi, M.A. Shokrgozar, B. Abd Emamy, J. Raush and M. Mahmoudi, *ACS Chem. Neurosci*., 2013, **4**, 375–378.
26 N. Taebnia, A. Arpanaei, D. Morshedi, S. Yaghmaie and F. Aliakbari, *Proc. of the 5th Conference on Nanostructures*, Kish Island, Iran, 2014.
27 C. Cabaleiro-Lago, O. Szczepankiewicz and S. Linse, *Langmuir*, 2012, **28**, 1852-1857.
28 V. Vigneswara, J.D. Lowenson, C.D. Powell, M. Thakur, K. Bailey, S. Clarke, D.E. Ray and W.G. Carter, *J. Biol. Chem*., 2006, **281**, 32619–32629.
29 J. Pronchik, X. He, J.T. Giurleo and D.S. Talaga, *J. Am. Chem. Soc.*, 2010, **132**, 9797-9803.
30 R. Vácha, S. Linse and M. Lund, *J. Am. Chem. Soc.*, 2014, **136(33)**, 11776-11782.